# MULTI-TASK STRUCTURAL LEARNING USING LOCAL TASK SIMILARITY INDUCED NEURON CREATION AND REMOVAL

**Anonymous authors**
Paper under double-blind review

## ABSTRACT

Multi-task learning has the potential to improve generalization by maximizing positive transfer between tasks while reducing task interference. Fully achieving this potential is hindered by manually designed architectures that remain static throughout training. On the contrary, learning in the brain occurs through structural changes that are in tandem with changes in synaptic strength. Therefore, we propose *Multi-Task Structural Learning (MTSL)* that simultaneously learns the multi-task architecture and its parameters. MTSL begins with an identical single task network for each task and alternates between a task learning phase and a structural learning phase. In the task learning phase, each network specializes in the corresponding task. In each of the structural learning phases, starting from the earliest layer, locally similar task layers first transfer their knowledge to a newly created group layer after which they become redundant and are removed. Our experimental results show that MTSL achieves competitive generalization with various baselines and improves robustness to out-of-distribution data. [1]

## 1 INTRODUCTION

Artificial Neural Networks (ANNs) have exhibited strong performance in various tasks essential for scene understanding. Single-Task Learning (STL) Yu et al. (2021); Orsic et al. (2019); Wang et al. (2020b) has been largely at the center of this exhibit driven by custom task-specific improvements. Despite these improvements, using single task networks for the multiple tasks required for scene understanding comes with notable problems such as a linear increase in computational cost and a lack of inter-task communication.

Multi-Task Learning (MTL), on the other hand, with the aid of shared layers provides favorable benefits over STL such as improved inference efficiency and positive information transfer between tasks. However, a notable drawback of sharing layers is task interference. Existing works have attempted to alleviate task interference using architecture modifications Liu et al. (2019); Kanakis et al. (2020), by determining which tasks to group together using a notion of similarity Standley et al. (2020); Fifty et al. (2021); Vandenhende et al. (2020), by balancing task loss functions Kendall et al. (2018); Liu et al. (2019); Yu et al. (2020); Lin et al. (2019), or by learning the architecture Guo et al. (2020); Lu et al. (2017). Although these methods have shown promise, progress can be made by drawing inspiration from the brain which is the only known intelligent system that excels in multi-task learning. The inner mechanisms of the brain, although not fully understood, can guide research in ANNs through simplified notions. Neuron creation and neuron removal Maile et al. (2022) are simplified notions that can aid the automated design of Multi-Task Networks (MTNs).

**Neuron removal** presents the opportunity to start from a dense set of neurons and move towards a sparse set of neurons. In the early stages of development in the brain, neural circuits consist of excess neurons and connections that provide a rich information pipeline Maile et al. (2022). This pipeline allows neural circuits to learn specialized functions while they undergo neuron removal and synaptic pruning Riccomagno & Kolodkin (2015). Thereby, moving from a dense architecture consisting of multiple single-task networks to a sparse multi-task architecture could be beneficial.

[1] Code will be made available after acceptance.

**Neuron creation** is an open-ended operation due to the difficulty involved in deciding where, how, and when to create neurons Evci et al. (2022). In the brain, local communication between neurons is an important part of learning. Learning rules that modulate synaptic strength are local in nature Kudithipudi et al. (2022) and local neural activity could be responsible for the creation of neurons Luhmann et al. (2016) and also neuron removal Faust et al. (2021). We explore local task similarity to drive neuron creation and removal which together could improve learning.

**Structural learning** pertains to the learning of the architecture and its parameters simultaneously Maile et al. (2022). The neural circuitry in the brain changes even during adulthood undergoing morphological changes induced by structural plasticity Kudithipudi et al. (2022). Evidently, learning in the brain does not involve static architecture creation followed by modulation of synaptic strengths. Instead, architecture changes happen in tandem with changes in synaptic strength. Thus, utilizing structural learning with strategic neural operations could mitigate the effects of task interference and promote generalization in MTL.

Therefore, we propose Multi-Task Structural Learning (MTSL) to simultaneously learn the multi-task architecture and its parameters. MTSL considers entire layers as the computation units Maile et al. (2022) and performs neuron creation and neuron removal on them. Inspired by the creation of a large number of neurons in the developmental stage of the brain, MTSL begins training by initializing each task with its own network. Similar to the brain, the excess layers of each task network provide a rich information flow to inform grouping decisions. Local task similarity is used to guide task learning through the alignment of task representations and also to make decisions on grouping tasks. A positive decision to group tasks induces the creation of a group layer and the associated task layers transfer their learned knowledge to the group layer before being removed. Finally, a few epochs of fine-tuning result in a learned MTN which persists the learned parameters for inference.

**Contributions**. (i) We propose a structural learning algorithm for multi-task learning based on aligning local task representations, grouping similar task layers, transferring information from grouped task layers to a new group layer and removing the concerned task layers. (ii) We compare against various state-of-the-art methods and show that MTSL shows improved generalization without the need to retrain. (iii) We show that MTSL improves robustness to natural corruptions. (iv). We present an ablation on the various components of MTSL and show its utility.

## 2 Related works

We consider a variety of existing works in the multi-task learning literature and discuss how MTSL is different. Other works that can help leverage neural operators have been discussed in Section A.

Although different lines of work such as architecture modifications Liu et al. (2019); Kanakis et al. (2020); Misra et al. (2016), task grouping Standley et al. (2020); Fifty et al. (2021); Vandenhende et al. (2020), or task loss balancing Kendall et al. (2018); Liu et al. (2019); Yu et al. (2020); Lin et al. (2019) address task interference, they use hand-designed architectures that might be sub-optimal. A variety of works in the MTL literature propose methods to learn the architecture and we categorize these works into two groups. One group of works consider learning architectures that are capable of dynamically changing their structure based on the input Hazimeh et al. (2021); Ahn et al. (2019); Rosenbaum et al. (2018) while the other group learns the branching structure Guo et al. (2020); Bruggemann et al. (2020); Lu et al. (2017); Zhang et al. (2022; 2021).

**Input dependent dynamic architectures** draw inspiration from the brain and provide many benefits including improved computational efficiency Han et al. (2021). DSelect-k Hazimeh et al. (2021) is a mixture of experts model that enables selecting a spare set of experts to infer an input sample. Ahn et al. (2019) learn a selector network that learns to pick a subnetwork from a large estimator network based on the input. In routing networks Rosenbaum et al. (2018), task dependent agents are trained using reinforcement learning to pick a path within a large network for inferring an input. While these approaches aim at optimizing networks or subnetworks to specialize for certain distribution of input samples, MTSL aims at optimizing a shared network for all tasks.

**The branching structure** of multi-task networks have been learned using different approaches. Zhang et al. (2022) propose to estimate the accuracy of a potential branched multi-task network with the help of two task networks with similar branching. They also suggest data structures and methods to ease search branching decisions in an arbitrary CNN similar to Zhang et al. (2021). Guo et al.

(2020) start from a dense search space where a child layer is connected to a number of parent layers. During learning, a distribution over parent nodes is learned with the aid of path sampling. At the end of training, a valid network path is picked and using neuron removal, the neurons no longer a part of the valid path are removed. BMTAS Bruggemann et al. (2020) takes a similar approach to Guo et al. (2020) but additionally use a resource loss. On the contrary, MTSL involves progressive neuron removals at different intervals during training. The branching structure learning approaches discussed so far explicitly retrain the learned architecture. MTSL avoids this retraining steps and confirms with structural learning. Like MTSL, Lu et al. (2017) also avoid retraining and use neuron creation where tasks are split into different branches starting from the output layer to the input layer using inter-task affinities defined based on task error margins. Unlike Lu et al. (2017), MTSL starts from a dense set of neurons and moves towards a sparse architecture. Also, MTSL is designed to leverage both neuron creation and neuron removal. Adashare Sun et al. (2020) learns task specific policies to determine which residual blocks to execute or skip, leading to residual blocks in the encoder specializing in a subset of tasks. Unlike Guo et al. (2020); Bruggemann et al. (2020); Zhang et al. (2022; 2021) and MTSL, Adashare does not directly learn a branching structure and is specifically designed for ResNet.

## 3 Multi-Task Structural Learning (MTSL)

The tasks to be learned together in an MTN bring in diverse information about the input scene. This diverse information can be leveraged to learn representations with improved generalization on all tasks. Design decisions such as which layers to share and where to branch tasks are complex due their combinatorial nature. This complexity along with the crucial role of these decisions in the interplay between positive transfer and task interference are reasons that could render manual architecture design sub-optimal. Structural learning on the other hand, learns the architecture along with its parameters which is likely in line with how the brain learns.

MTSL utilizes two neural operators namely neuron creation and neuron removal to aid in structural learning. In early development, the brain has excess neurons that can provide a rich information pipeline for a pruned neural circuit to functionally specialize. Likewise, MTSL creates excess neurons by starting from a disparate network for each task. Through the progress of training, corresponding task neurons in a layer pave the way for a specialized group neuron leading to a structural change. In the upcoming sections we present the finer details of the MTSL algorithm. In Section 3.1, we formalize the problem setup and establish terminologies that we use in the rest of the paper. Following this section, we discuss how we align task representations in Section 3.2, how we create neurons in Section 3.3, removal of task neurons in Section 3.4 and the overall MTSL algorithm in Section 3.5.

### 3.1 Problem Setup

We consider the problem of structural learning where the MTN architecture and its parameters are learned simultaneously. Given the set of $\mathcal{T}$ tasks that each has its own single network with $L$ layers, our algorithm results in a single MTN capable of inferring all the $\mathcal{T}$ tasks accurately without any need for retraining. First, we establish the terminologies that are used in the rest of the paper. A **node** is a layer that connects one branch to another branch (or to a node) and a **branch** is a sequence of layers that follow a node. Initially, the first layer of each single task network is the task node while the rest of the task network excluding the task head is called the task branch. Similarly, a group of tasks will have a group node and a group branch. A task node is of particular significance to our algorithm as tasks can be only fused at the task node. Also, only the task nodes which are connected to the same group branch or group node can be fused. At the start of the training, all task nodes are connected to the input image and can be fused. $T$ and $G$ denote a task and a group, respectively. Additionally, $F$ and $\mathcal{F}$ denote the output features of task node and group node, respectively. Figure 1 provides the overall schematic of our approach where the leftmost column illustrates the initial state of our setup making use of the terminologies defined so far. In the upcoming sections, we discuss the different components of our approach.

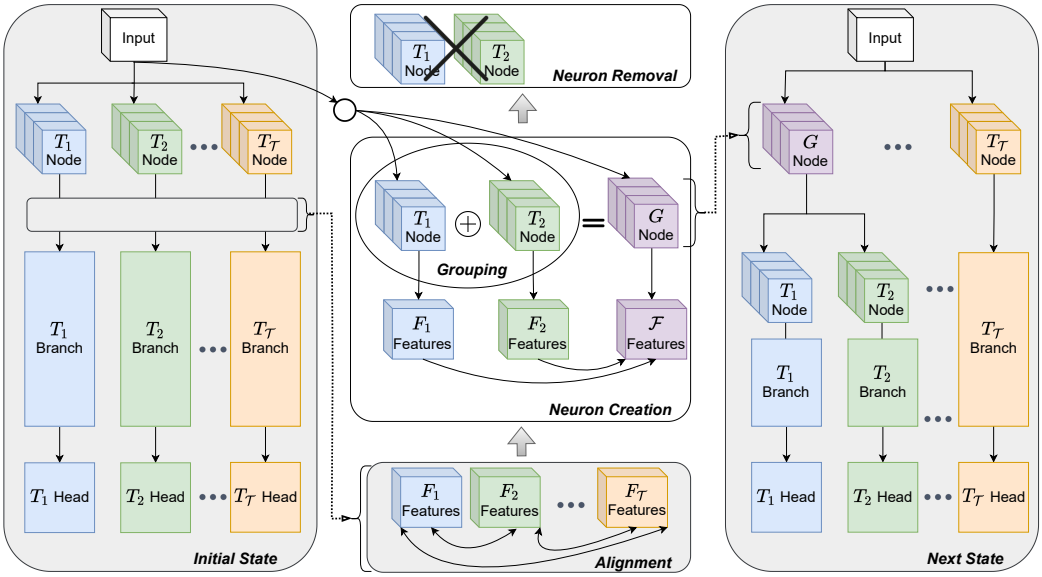


Figure 1: Schematic of the MTSL Algorithm. The grey regions (initial state, alignment, next state) are part of the task learning phase while the white regions (neuron creation, and neuron removal) are part of the structural learning phase. During training, our algorithm loops between alignment in the task learning phase followed by neuron creation and neuron removal in the structural learning phase leading to the next state (last column).

### 3.2 Aligning Task Specific Representations

As is evident from Figure 1, we begin training from single task networks. Since the encoder of each task is initialized with ImageNet weights, there exists a correspondence between task nodes initially. During training, the task nodes would learn concepts that minimize the particular task loss independent of other tasks. This independence likely breaks any correspondence between parameters mapped one-to-one between any two task nodes. This behaviour comes from the permutation invariance of neural networks leading to no guarantee concerning the order in which concepts are learned Wang et al. (2020a). Therefore, MTSL aligns the concepts learned by task nodes and locally increases their similarity using Centered Kernel Alignment (CKA) Kornblith et al. (2019).

CKA is used to measure the similarity between two feature representations and has been shown to provide meaningful similarity scores. During training, we introduce a CKA-based regularization term between task nodes branching from the same group node/branch (or the input). This regularization term, as shown in the alignment part of Figure 1, is included between all pairs of task node features (indicated using bi-directional arrows) and enforces the task representations to align by serving as an alignment constraint. We use the unbiased CKA estimator Nguyen et al. (2021) to facilitate reliable estimates of CKA with small batch sizes used during training.

$$\mathcal{L} = \mathcal{L}_{MTL} - \lambda \mathcal{L}_{CKA} \tag{1}$$

The overall loss that is used for training in the task learning phase of our algorithm, is provided in Equation 1. Where the first term represents the multi-task loss which is a weighted sum of all individual task losses and the CKA regularization term is included with a balancing factor $\lambda$ and with a negative sign to maximize alignment between tasks.

### 3.3 Creating Group Nodes

The overall loss $\mathcal{L}$ used during the task learning phase (discussed in Section 3.2) leads tasks to learn similar features while also minimizing the concerned task loss. After the task learning phase, MTSL begins the structural learning phase to first leverage neuron creation. In the brain, local neuronal activity can affect the structure of the neural circuitry Luhmann et al. (2016) and play a role in learning experiences Kudithipudi et al. (2022). Taking cues from these notions of locality, we use

CKA to gauge the similarity between task node features that represent the local activity of task neurons. These local task similarities are used to induce the creation of group nodes.

First, CKA between all pairs of task node features is calculated after which all possible groups of task nodes are listed. From these groups, a set of groups that maximizes the total similarity is picked and the groups that satisfy a minimum similarity of $\gamma$ induce the creation of a group neuron. For instance, in Figure 1, we see that the groups picked are $[T_1, T_2]$ and $T_3$ assuming that the total number of tasks $\mathcal{T}$ is three. More details regarding the grouping algorithm are provided in the Appendix.

After task nodes have been grouped based on local task similarity, for each group a group node is created. The learned knowledge in the task neurons is used to initialize the created group node using a two-step process. In the first step, the weights of the group node are obtained by averaging the parameters of the concerned task nodes. This averaging is justified by the alignment constraint used in the task learning phase that ensures that corresponding parameters learn similar concepts. Figure 1 depicts the averaging initialization using a plus symbol. In the second step, MTSL distills the information learned by multiple task nodes into the group node using an attention-based feature amalgamation method Ye et al. (2019) referred to as **ATT**. Figure 1 depicts this amalgamation process by using arrows from task node features $F_1$ and $F_2$ to group node feature $\mathcal{F}$.

$$\mathcal{L}_{KA} = \frac{1}{N} \sum_{i}^{N} \left( F_i - ATT_i^{net}(\mathcal{F}) * \mathcal{F} \right)^2 \tag{2}$$

The knowledge amalgamation objective $\mathcal{L}_{KA}$ is provided in Equation 2 assuming that there are $N$ tasks grouped together. $ATT^{net}$ denotes the attention network consisting of two linear layers with an intermediate ReLU activation and a final sigmoid activation.

### 3.4 Removing Task Neurons

Starting from a dense set of neurons as in the initial state of MTSL provides the opportunity to leverage a rich information flow originating from diverse task information. Using neuron removal, MTSL moves towards a sparser architecture by removing task nodes that learn similar representations. These locally similar task nodes become redundant once they transfer their knowledge to the group node. The task branch is then disconnected from these redundant task nodes and connected to the group node. As defined in Section 3.1, the neurons from the task branch that now connect to the group node become the task nodes. These changes are evident in the depicted next state in Figure 1.

### 3.5 MTSL Algorithm

Algorithm 1 presents the different phases involved in the MTSL algorithm, namely the task learning phase, the structural learning phase, and a fine-tuning phase. The task learning phase and structural learning phase occur alternatively for $n$ number of times followed by a final fine-tuning phase. In the task learning phase, the entire network is trained to minimize the multi-task loss and maximize similarity among task nodes as described in Section 3.2. The structural learning phase involves neuron creation and neuron removal as discussed in Section 3.3 and in Section 3.4, respectively. $E_t$ determines the number of epochs for which each subsequent task learning phase is executed. Similarly, $E_s$ determines the epochs for ATT-based knowledge transfer. Considering a total training budget of $E$ epochs, the task learning phase is executed up to $E - f$ epochs where $f$ is the minimum epochs allocated for the fine-tuning phase during which the task nodes are no longer forced to align.

## 4 Experiments

We evaluate the strengths of our approach using two datasets, namely **Cityscapes** Cordts et al. (2016) and **NYUv2** Silberman et al. (2012). The Cityscapes dataset is an outdoor driving scenes dataset consisting of 2975 training images and 500 validation images. The images are reshaped to a resolution of 256×512 both in training and validation. The NYUv2 dataset consists of indoor scenes with a total of 795 training and 654 validation images, respectively. Cityscapes and NYUv2 datasets are also referred to as CS and NYU, respectively. We consider five dense prediction tasks, namely semantic segmentation ($\mathcal{S}$), depth estimation ($\mathcal{D}$), edge detection ($\mathcal{E}$), surface normals ($\mathcal{N}$) and autoencoder ($\mathcal{A}$). All numbers are reported on the validation set of each dataset as an average over three runs.

**Algorithm 1:** MTSL algorithm

**Input:** Initial state (as depicted in Figure 1), Training budget $E$, Minimum fine-tuning budget $f$;
$n \leftarrow$ Number of structural learning phases;
Task Learning Epochs $E_t \leftarrow [t^1, t^2.., t^n]$, $\sum_i^n E_t^i < E - f$;
Structural Learning Epochs $E_s \leftarrow [s^1, s^2.., s^n]$;
**while** $e < E - f$ **do**
  $t \leftarrow$ Next value from $E_t$; `// Task Learning Phase`
  **for** $t$ epochs **do**
    Train using loss $\mathcal{L}$ in Equation 1;
  **end**
  $e \leftarrow e + t$;
  Create group nodes using local task similarity; `// Structural Learning Phase`
  Average corresponding task nodes to initialize group nodes;
  $s \leftarrow$ Next value from $E_s$;
  **for** $s$ epochs **do**
    Use ATT to transfer knowledge in corresponding task nodes to group nodes;
  **end**
  **if** there is no more layer in all task branches **then**
    Exit loop;
  **end**
**end**
**for** $E - e$ epochs **do** `// Fine-Tuning Phase`
  Fine-tune using multi-task loss $\mathcal{L}_{MTL}$;
**end**

Each of the experiments have been run on one Nvidia Tesla V100 GPU in a DGX cluster. Additional training details can be found in Section C in the Appendix.

We provide multi-task performance improvement Vandenhende et al. (2021) using Equation 3 where $m$ and $s$ represent task performance in multi-task and single-task networks, respectively. When higher performance is better as for segmentation, $l$ is 0 and when lower performance is better $l$ is 1. We also report multi-task performance improvements in segmentation $\mathcal{S}$ and depth $\mathcal{D}$ tasks as $\Delta_{MTL}^{\mathcal{SD}}$,

$$\Delta_{MTL} = \frac{1}{T} \sum_{i=1}^{T} (-1)^{l_i} \left( M_{m,i} - M_{s,i} \right) / M_{s,i} \tag{3}$$

We compare MTSL with state-of-the-art methods (Section 4.1), evaluate the generalization, inference efficiency (Section 4.2), and robustness of MTSL (Section 4.3). We draw insights based on the converged network architecture in Section 4.4 and provide a detailed ablation study in Section 4.5.

### 4.1 Comparison with state-of-the-art methods

We compare MTSL with existing multi-task architectures and methods to learn multi-task architecture branching. Implementations of Cross-stitch Misra et al. (2016) and MTAN Liu et al. (2019) have been taken from the repository of Vandenhende et al. (2021) while the implementation of Learning-to-Branch (LTB) Guo et al. (2020) has been taken from LibMTL Lin & Zhang (2022). We update LTB with the resource loss proposed by BMTAS from their open source repository to obtained the implementation of BMTAS. LTB-R and BMTAS-R refer to the results obtained by retraining the converged architecture from scratch[2]. For all methods we use the same hyperparameter settings and use ResNet18 backbone with DeepLab head.

In Table 1, we observe that Cross-stitch obtains the best improvement over STN (highlighted in bold). As Cross-stitch retains all the separate task networks and learns adapter parameters to enable

[2]Encoder initialized with ImageNet weights and decoder randomly initialized.

Table 1: Generalization and inference efficiency comparisons between MTSL and state-of-the-art methods namely Cross-stitch Misra et al. (2016), MTAN Liu et al. (2019), LTB Guo et al. (2020) and BMTAS Bruggemann et al. (2020). LTB-R and BMTAS-R represent results obtained by retraining the final converged architecture of LTB and BMTAS, respectively. # (M) denotes the number of parameters in millions.

| | CS | | | | NYU | | | |
|---|---|---|---|---|---|---|---|---|
| Network | $\Delta_{MTL}^{\mathcal{SD}} \uparrow$ | $\Delta_{MTL} \uparrow$ | # (M) | GMac | $\Delta_{MTL}^{\mathcal{SD}} \uparrow$ | $\Delta_{MTL} \uparrow$ | # (M) | GMac |
| STN | - | - | 79.50 | 26.73 | - | - | 79.51 | 29.24 |
| One-Net | -0.84$_{\pm 0.15}$ | -1.22$_{\pm 0.04}$ | 34.79 | 7.70 | -0.79$_{\pm 0.11}$ | -4.57$_{\pm 0.13}$ | 34.80 | 8.42 |
| Cross-stitch | **+2.79**$_{\pm 0.41}$ | **+1.01**$_{\pm 0.17}$ | 79.50 | 26.73 | **+0.73**$_{\pm 0.37}$ | -2.18$_{\pm 0.25}$ | 79.53 | 29.24 |
| MTAN | -0.02$_{\pm 0.49}$ | -3.68$_{\pm 0.64}$ | 36.61 | 11.13 | -0.34$_{\pm 0.93}$ | -3.91$_{\pm 0.54}$ | 36.62 | 12.18 |
| LTB-R | +0.49$_{\pm 0.40}$ | +0.11$_{\pm 0.17}$ | 68.15 | 19.81 | -0.13$_{\pm 0.10}$ | -0.23$_{\pm 0.08}$ | 79.17 | 25.20 |
| BMTAS-R | +0.25$_{\pm 0.57}$ | -0.02$_{\pm 0.26}$ | 68.30 | 21.03 | -0.10$_{\pm 0.29}$ | **-0.21**$_{\pm 0.28}$ | 79.17 | 25.20 |
| LTB | -2.95$_{\pm 0.42}$ | -1.79$_{\pm 0.18}$ | 68.15 | 19.81 | -4.78$_{\pm 0.40}$ | -5.35$_{\pm 0.31}$ | 79.17 | 25.20 |
| BMTAS | -3.84$_{\pm 0.39}$ | -2.19$_{\pm 0.11}$ | 68.30 | 21.03 | -4.00$_{\pm 0.74}$ | -5.07$_{\pm 0.42}$ | 79.17 | 25.20 |
| MTSL | <u>-0.23</u>$_{\pm 0.85}$ | <u>-0.34</u>$_{\pm 0.37}$ | 68.37 | 12.00 | <u>-0.06</u>$_{\pm 0.34}$ | <u>-3.21</u>$_{\pm 0.21}$ | 59.98 | 11.95 |

information transfer between tasks. While comparing MTSL with methods that learn branching structures (last group), MTSL outperforms both LTB and BMTAS by a considerable margin in both datasets. For instance, in $\Delta_{MTL}^{\mathcal{SD}}$, MTSL outperforms LTB by 2.72 % and 4.72 % and BMTAS by 3.61 % and 3.94 % in Cityscapes and NYUv2 datasets while requiring lower GMac. LTB-R and BMTAS-R outperform MTSL in Cityscapes but at the cost of retraining and deviating from structural learning. Overall, we note that MTSL holds the potential to simultaneously learn the architecture and its parameter while being competitive in performance and inference efficiency.

The methods discussed so far only consider learning branching structure in the encoder. For the upcoming experiments, we extend MTSL to an encoder-decoder architecture with a total of ten locations, six in the encoder and four in the decoder where task nodes can participate in neuron creation and removal. The encoder consists of a ResNet18 based backbone and the decoder is also based on ResNet blocks.

### 4.2 Generalization and Inference Efficiency

MTSL algorithm begins from single task networks (**STN**s) and potentially could end in a network with all the encoder and decoder layers shared between all tasks (we refer to as **One-Net**). These two possible networks are considered as the baselines to evaluate our approach. Table 2 shows the generalization performance of the baselines and MTSL. We see that MTSL achieves better generalization than One-Net in most cases while being close to One-Net in inference efficiency as is evident from the columns for GMac and number of parameters. In NYUv2, MTSL even rivals the performance of STN in both $\mathcal{S}$ and $\mathcal{D}$ tasks. The improved generalization can be attributed to the brain-inspired aspects of the MTSL algorithm such as local task similarity and dense to sparse change of the architecture.

The training time of MTSL is higher than that of One-Net because of the training epochs required for knowledge amalgamation. However, this only adds 34 additional epochs in training where only the network parts up until the task nodes is involved in the computation. For a fair comparison, we train One-Net for 34 more epochs and get the One-Net-L baseline. We note that MTSL also improves generalization over One-Net-L. Overall, we see that with only a fractional increase in training costs, MTSL algorithm provides a learned network with better generalization.

### 4.3 Robustness to Natural Corruptions

MTSL provides improved generalization likely due to its motivation originating from abstract notions of the brain. Given that the brain is effective in discerning noise from semantics, a natural question to ask is whether MTSL can lead to improvements in robustness to natural corruptions. Table

Table 2: Generalization and inference efficiency comparisons between MTSL and the baselines. MTSL performs better than One-Net in most cases and achieves an inference efficiency close to One-Net. # (M) denotes the number of parameters in millions.

| | Network | $\mathcal{S} \uparrow$ | $\mathcal{D} \downarrow$ | $\mathcal{E} \downarrow$ | $\mathcal{N} \uparrow$ | $\mathcal{A} \downarrow$ | $\Delta_{MTL}^{\mathcal{SD}} \uparrow$ | $\Delta_{MTL} \uparrow$ | # (M) | GMac |
|---|---|---|---|---|---|---|---|---|---|---|
| CS | STN | $60.87_{\pm 0.78}$ | $6.37_{\pm 0.02}$ | $0.03_{\pm 0.00}$ | $0.61_{\pm 0.00}$ | $0.05_{\pm 0.00}$ | - | - | 107.10 | 31.03 |
| | One-Net | $60.34_{\pm 0.37}$ | $6.76_{\pm 0.04}$ | $\mathbf{0.04}_{\pm 0.00}$ | $0.59_{\pm 0.00}$ | $\mathbf{0.06}_{\pm 0.00}$ | $-3.47_{\pm 0.80}$ | $-9.65_{\pm 0.46}$ | 21.70 | 7.06 |
| | One-Net-L | $60.71_{\pm 0.21}$ | $6.75_{\pm 0.03}$ | $\mathbf{0.04}_{\pm 0.00}$ | $0.59_{\pm 0.00}$ | $\mathbf{0.06}_{\pm 0.00}$ | $-3.15_{\pm 0.62}$ | $-9.39_{\pm 0.57}$ | 21.70 | 7.06 |
| | MTSL | $\mathbf{60.68}_{\pm 0.10}$ | $\mathbf{6.52}_{\pm 0.03}$ | $\mathbf{0.04}_{\pm 0.00}$ | $\mathbf{0.60}_{\pm 0.00}$ | $\mathbf{0.06}_{\pm 0.00}$ | $\mathbf{-1.35}_{\pm 0.70}$ | $\mathbf{-7.04}_{\pm 0.56}$ | 22.86 | 8.96 |
| NYU | STN | $35.63_{\pm 0.53}$ | $52.70_{\pm 0.25}$ | $0.06_{\pm 0.00}$ | $0.80_{\pm 0.00}$ | $0.14_{\pm 0.00}$ | - | - | 107.10 | 33.99 |
| | One-Net | $34.15_{\pm 0.15}$ | $53.44_{\pm 0.39}$ | $\mathbf{0.06}_{\pm 0.00}$ | $\mathbf{0.74}_{\pm 0.00}$ | $0.17_{\pm 0.01}$ | $-2.77_{\pm 0.88}$ | $-9.82_{\pm 1.87}$ | 21.70 | 7.77 |
| | One-Net-L | $34.42_{\pm 0.17}$ | $53.36_{\pm 0.31}$ | $\mathbf{0.06}_{\pm 0.00}$ | $\mathbf{0.74}_{\pm 0.00}$ | $0.17_{\pm 0.01}$ | $-2.77_{\pm 0.70}$ | $-9.82_{\pm 1.67}$ | 21.70 | 7.77 |
| | MTSL | $\mathbf{35.50}_{\pm 0.25}$ | $\mathbf{52.46}_{\pm 0.23}$ | $\mathbf{0.06}_{\pm 0.00}$ | $0.73_{\pm 0.00}$ | $\mathbf{0.16}_{\pm 0.00}$ | $\mathbf{+0.06}_{\pm 1.03}$ | $\mathbf{-6.21}_{\pm 0.90}$ | 22.81 | 9.89 |

Table 3: Robustness to natural corruptions under four categories. MTSL shows better robustness compared to One-Net in most cases.

| | Network | $\Delta_{MTL}^{\mathcal{SD}} \uparrow$ | | | | $\Delta_{MTL} \uparrow$ | | | |
|---|---|---|---|---|---|---|---|---|---|
| | | Noise | Blur | Weather | Digital | Noise | Blur | Weather | Digital |
| CS | One-Net | -5.78 | -1.32 | -3.81 | -2.15 | **+3.02** | -7.73 | -1.36 | -12.22 |
| | MTSL | **-3.03** | **+0.21** | **+0.49** | **+1.42** | +2.92 | **-3.72** | **+2.60** | **-7.07** |
| NYU | One-Net | **+10.25** | -3.71 | -3.27 | -2.72 | **+15.72** | -8.51 | -11.79 | -10.35 |
| | MTSL | +1.92 | **-2.65** | **-0.84** | **-1.14** | +13.50 | **-8.03** | **+3.22** | **-7.54** |

3 shows the robustness of the baselines and MTSL to various natural corruptions Hendrycks & Dietterich (2019) categorized under four types, namely noise, blur, weather, and digital. Under each corruption category, the average across five different severity levels is taken. We see that the MTSL network exhibits better robustness compared to One-Net in most cases, especially in the weather and digital category of the Cityscapes dataset. These results further demonstrate that MTSL presents a compelling case for the utility of drawing inspirations from the brain.

### 4.4 Converged Network Architecture and Task Groups

Assumptions about the data used for training play a pivotal role in determining the learned representations. In the brain, exposure to the nature of experiences determines the way in the which the neural circuitry develops Kudithipudi et al. (2022). Thus, the resultant architecture obtained with MTSL on two datasets would likely differ. Figure 2 visualizes the One-Net architecture and the learned architectures in Cityscapes and NYUv2. Evidently, after the first branch from layer six, the task groups and the branching structure emerging on the two datasets are different. Semantic segmentation ($\mathcal{S}$) and edge detection ($\mathcal{E}$) being grouped together in both datasets follows intuition as edge detection requires predictions of semantic edges. However, the emergence of certain groups of tasks such as depth and autoencoder in NYUv2 is counter-intuitive. In addition to task relationships, these results show that local task similarity and inherent biases in the dataset can also impact the optimal architecture. In Section D, we analyze the sensitivity of the converged architecture to random seeds and initialization.

### 4.5 Ablation Study

To determine the effectiveness of the different components involved in MTSL, we perform systematic evaluations and provide the results in Table 4. When alignment is not used, the task representations largely diverge around layers three and four. As a result, task nodes no longer become sufficiently similar to be fused. Therefore, the resultant architectures in the first three rows perform similarly and have inference requirements close to STN. On the other hand, in the last three rows, with the help of alignment, the resultant architectures undergo neuron creation and removal in more layers and approach close to the inference efficiency of One-Net. Out of these, the last row constitutes all the

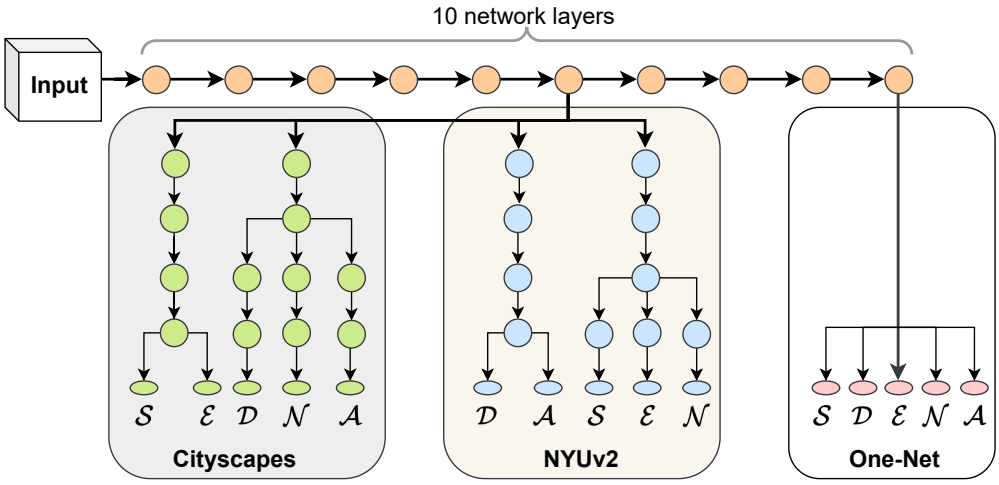


Figure 2: Visualization of the One-Net architecture and the MTSL resultant architectures. In both datasets, tasks branch out at layer six but differences emerge in the branching structure in the following layers. The oval shapes at the end of each path represents the task heads.

Table 4: Effect of alignment (Align), average initialization (Avg), and attention based knowledge amalgamation (ATT). In the first three rows, without alignment, the resultant networks remain close to STN. In the last three rows, alignment results in networks closer to One-Net.

| | | | CS | | | | NYU | | | |
|---|---|---|---|---|---|---|---|---|---|---|
| Align | Avg | ATT | $\Delta_{MTL}^{\mathcal{SD}} \uparrow$ | $\Delta_{MTL} \uparrow$ | # (M) | GMac | $\Delta_{MTL}^{\mathcal{SD}} \uparrow$ | $\Delta_{MTL} \uparrow$ | # (M) | GMac |
| | ✓ | | -0.35 | -2.25 | 97.37 | 17.02 | +0.38 | -4.24 | 69.94 | 17.87 |
| | | ✓ | -0.05 | -1.92 | 97.37 | 17.02 | +0.57 | -4.23 | 95.97 | 17.87 |
| | ✓ | ✓ | -0.39 | -2.12 | 95.97 | 16.30 | +0.31 | -4.25 | 95.97 | 17.87 |
| ✓ | ✓ | | -2.29 | -7.67 | 22.56 | 8.71 | -1.26 | -6.68 | 22.97 | 10.32 |
| ✓ | | ✓ | -3.62 | -9.66 | **22.51** | **8.60** | -2.36 | -6.71 | 23.10 | 10.90 |
| ✓ | ✓ | ✓ | **-1.35** | **-7.04** | 22.86 | 8.96 | **+0.06** | **-6.21** | **22.81** | **9.89** |

components used in MTSL and results in the best performance. Note that although we use CKA for alignment and attention for knowledge amalgamation, various other methods can also be used.

## 5 Conclusion

Inspired by the notion that both the structure of the neural circuits and the associated synaptic strengths change together in the brain, we proposed *Multi-Task Structural Learning (MTSL)*. MTSL relies on local similarity-induced creation of group neurons and removal of task neurons. We showed that MTSL results in networks with improved generalization and robustness while improving the inference efficiency. We discussed the dependence of the converged network architectures on local task similarity and the dataset. We studied the role of the different components in MTSL and found that enforcing local task similarities results in architectures with better inference efficiency.

**Limitations.** A fixed epoch schedule is used to transition between different learning phases of MTSL. Instead, automatically determining periods in training where structural learning is required can be explored. On this regard, the local inter-neuron activity in the brain could provide useful cues to automatically drive structural changes. Further, local similarity should likely be an emergent result of inter-neuron activity contrary to being explicitly enforced as in MTSL. MTSL does not use synaptogenesis and synaptic pruning thereby limiting its ability to learn connections. Despite these limitations, MTSL serves as an indication of the potential of extending simplified notions from neuroscience into multi-task learning.

## REFERENCES


Chanho Ahn, Eunwoo Kim, and Songhwai Oh. Deep elastic networks with model selection for multi-task learning. In *Proceedings of the IEEE/CVF International Conference on Computer Vision (ICCV)*, October 2019.

David Bruggemann, Menelaos Kanakis, Stamatios Georgoulis, and Luc Van Gool. Automated search for resource-efficient branched multi-task networks. In *BMVC*, 2020.

Marius Cordts, Mohamed Omran, Sebastian Ramos, Timo Rehfeld, Markus Enzweiler, Rodrigo Benenson, Uwe Franke, Stefan Roth, and Bernt Schiele. The cityscapes dataset for semantic urban scene understanding. In *Proc. of the IEEE Conference on Computer Vision and Pattern Recognition (CVPR)*, 2016.

Utku Evci, Bart van Merrienboer, Thomas Unterthiner, Fabian Pedregosa, and Max Vladymyrov. Gradmax: Growing neural networks using gradient information. In *International Conference on Learning Representations*, 2022. URL https://openreview.net/forum?id=qjN4h_wwUO.

Travis E Faust, Georgia Gunner, and Dorothy P Schafer. Mechanisms governing activity-dependent synaptic pruning in the developing mammalian cns. *Nature Reviews Neuroscience*, 22(11):657–673, 2021.

Christopher Fifty, Ehsan Amid, Zhe Zhao, Tianhe Yu, Rohan Anil, and Chelsea Finn. Efficiently identifying task groupings for multi-task learning. In A. Beygelzimer, Y. Dauphin, P. Liang, and J. Wortman Vaughan (eds.), *Advances in Neural Information Processing Systems*, 2021. URL https://openreview.net/forum?id=hqDb8d65Vfh.

Pengsheng Guo, Chen-Yu Lee, and Daniel Ulbricht. Learning to branch for multi-task learning. In Hal Daumé III and Aarti Singh (eds.), *Proceedings of the 37th International Conference on Machine Learning*, volume 119 of *Proceedings of Machine Learning Research*, pp. 3854–3863. PMLR, 13–18 Jul 2020. URL https://proceedings.mlr.press/v119/guo20e.html.

Yizeng Han, Gao Huang, Shiji Song, Le Yang, Honghui Wang, and Yulin Wang. Dynamic neural networks: A survey. *IEEE transactions on pattern analysis and machine intelligence*, PP, 2021.

Hussein Hazimeh, Zhe Zhao, Aakanksha Chowdhery, Maheswaran Sathiamoorthy, Yihua Chen, Rahul Mazumder, Lichan Hong, and Ed Chi. DSelect-k: Differentiable selection in the mixture of experts with applications to multi-task learning. In A. Beygelzimer, Y. Dauphin, P. Liang, and J. Wortman Vaughan (eds.), *Advances in Neural Information Processing Systems*, 2021. URL https://openreview.net/forum?id=tKlYQJLYN8v.

Xiaoxi He, Zimu Zhou, and Lothar Thiele. Multi-task zipping via layer-wise neuron sharing. In *NeurIPS*, 2018.

Dan Hendrycks and Thomas Dietterich. Benchmarking neural network robustness to common corruptions and perturbations. *Proceedings of the International Conference on Learning Representations*, 2019.

Menelaos Kanakis, David Bruggemann, Suman Saha, Stamatios Georgoulis, Anton Obukhov, and Luc Van Gool. Reparameterizing convolutions for incremental multi-task learning without task interference. In Andrea Vedaldi, Horst Bischof, Thomas Brox, and Jan-Michael Frahm (eds.), *Computer Vision – ECCV 2020*, pp. 689–707, Cham, 2020. Springer International Publishing. ISBN 978-3-030-58565-5.

Alex Kendall, Yarin Gal, and Roberto Cipolla. Multi-task learning using uncertainty to weigh losses for scene geometry and semantics. *2018 IEEE/CVF Conference on Computer Vision and Pattern Recognition*, pp. 7482–7491, 2018.

Simon Kornblith, Mohammad Norouzi, Honglak Lee, and Geoffrey Hinton. Similarity of neural network representations revisited. In Kamalika Chaudhuri and Ruslan Salakhutdinov (eds.), *Proceedings of the 36th International Conference on Machine Learning*, volume 97 of *Proceedings of Machine Learning Research*, pp. 3519–3529. PMLR, 09–15 Jun 2019. URL https://proceedings.mlr.press/v97/kornblith19a.html.

Dhireesha Kudithipudi, Mario Aguilar-Simon, Jonathan Babb, Maxim Bazhenov, Douglas Blackiston, Josh Bongard, Andrew P Brna, Suraj Chakravarthi Raja, Nick Cheney, Jeff Clune, et al. Biological underpinnings for lifelong learning machines. *Nature Machine Intelligence*, 4(3):196–210, 2022.

Alexey Kurakin, Ian J. Goodfellow, and Samy Bengio. Adversarial examples in the physical world. In *5th International Conference on Learning Representations, ICLR 2017, Toulon, France, April 24-26, 2017, Workshop Track Proceedings*. OpenReview.net, 2017. URL https://openreview.net/forum?id=HJGU3Rodl.

Mikhail Iu. Leontev, Viktoriia Islenteva, and Sergey V. Sukhov. Non-iterative knowledge fusion in deep convolutional neural networks. *Neural Processing Letters*, 51:1–22, 2019.

Wei-Hong Li and Hakan Bilen. Knowledge distillation for multi-task learning. In *Proceedings of the European Conference on Computer Vision Workshop on Imbalance Problems in Computer Vision*, 2020.

Baijiong Lin and Yu Zhang. LibMTL: A python library for multi-task learning. *arXiv preprint arXiv:2203.14338*, 2022.

Xi Lin, Hui-Ling Zhen, Zhenhua Li, Qing-Fu Zhang, and Sam Kwong. Pareto multi-task learning. In H. Wallach, H. Larochelle, A. Beygelzimer, F. d'Alché-Buc, E. Fox, and R. Garnett (eds.), *Advances in Neural Information Processing Systems*, volume 32. Curran Associates, Inc., 2019. URL https://proceedings.neurips.cc/paper/2019/file/685bfde03eb646c27ed565881917c71c-Paper.pdf.

Shikun Liu, Edward Johns, and Andrew J. Davison. End-to-end multi-task learning with attention. *2019 IEEE/CVF Conference on Computer Vision and Pattern Recognition (CVPR)*, pp. 1871–1880, 2019.

Yongxi Lu, Abhishek Kumar, Shuangfei Zhai, Yu Cheng, Tara Javidi, and Rogerio Feris. Fully-adaptive feature sharing in multi-task networks with applications in person attribute classification. In *2017 IEEE Conference on Computer Vision and Pattern Recognition (CVPR)*, pp. 1131–1140, 2017. doi: 10.1109/CVPR.2017.126.

Heiko J Luhmann, Anne Sinning, Jenq-Wei Yang, Vicente Reyes-Puerta, Maik C Stüttgen, Sergei Kirischuk, and Werner Kilb. Spontaneous neuronal activity in developing neocortical networks: from single cells to large-scale interactions. *Frontiers in neural circuits*, 10:40, 2016.

Sihui Luo, Xinchao Wang, Gongfan Fang, Yao Hu, Dapeng Tao, and Mingli Song. Knowledge amalgamation from heterogeneous networks by common feature learning. In *Proceedings of the 28th International Joint Conference on Artificial Intelligence (IJCAI)*, 2019.

Sihui Luo, Wenwen Pan, Xinchao Wang, Dazhou Wang, Haihong Tang, and Mingli Song. Collaboration by competition: Self-coordinated knowledge amalgamation for multi-talent student learning. In *ECCV*, 2020.

Aleksander Madry, Aleksandar Makelov, Ludwig Schmidt, Dimitris Tsipras, and Adrian Vladu. Towards deep learning models resistant to adversarial attacks. In *International Conference on Learning Representations*, 2018. URL https://openreview.net/forum?id=rJzIBfZAb.

Kaitlin Maile, Luga Hervé, and Dennis George Wilson. Structural learning in artificial neural networks: A neural operator perspective. *Transactions on Machine Learning Research*, 2022. URL https://openreview.net/forum?id=gzhEGhcsnN. Survey Certification.

I. Misra, Abhinav Shrivastava, A. Gupta, and M. Hebert. Cross-stitch networks for multi-task learning. *2016 IEEE Conference on Computer Vision and Pattern Recognition (CVPR)*, pp. 3994–4003, 2016.

Thao Nguyen, Maithra Raghu, and Simon Kornblith. Do wide and deep networks learn the same things? uncovering how neural network representations vary with width and depth. In *International Conference on Learning Representations*, 2021. URL https://openreview.net/forum?id=KJNcAkY8tY4.

Marin Orsic, Ivan Kreso, Petra Bevandic, and Sinisa Segvic. In defense of pre-trained imagenet architectures for real-time semantic segmentation of road-driving images. In *Proceedings of the IEEE/CVF Conference on Computer Vision and Pattern Recognition*, pp. 12607–12616, 2019.

Martin M Riccomagno and Alex L Kolodkin. Sculpting neural circuits by axon and dendrite pruning. *Annual review of cell and developmental biology*, 31:779–805, 2015.

Clemens Rosenbaum, Tim Klinger, and Matthew Riemer. Routing networks: Adaptive selection of non-linear functions for multi-task learning. In *International Conference on Learning Representations*, 2018. URL https://openreview.net/forum?id=ry8dvM-R-.

Chengchao Shen, Xinchao Wang, Jie Song, Li Sun, and Mingli Song. Amalgamating knowledge towards comprehensive classification. In *Proceedings of the Thirty-Third AAAI Conference on Artificial Intelligence and Thirty-First Innovative Applications of Artificial Intelligence Conference and Ninth AAAI Symposium on Educational Advances in Artificial Intelligence*, AAAI'19/IAAI'19/EAAI'19. AAAI Press, 2019. ISBN 978-1-57735-809-1. doi: 10.1609/aaai.v33i01.33013068. URL https://doi.org/10.1609/aaai.v33i01.33013068.

N. Silberman, Derek Hoiem, P. Kohli, and R. Fergus. Indoor segmentation and support inference from rgbd images. In *ECCV*, 2012.

Sidak Pal Singh and Martin Jaggi. Model fusion via optimal transport. In H. Larochelle, M. Ranzato, R. Hadsell, M. F. Balcan, and H. Lin (eds.), *Advances in Neural Information Processing Systems*, volume 33, pp. 22045–22055. Curran Associates, Inc., 2020. URL https://proceedings.neurips.cc/paper/2020/file/fb2697869f56484404c8ceee2985b01d-Paper.pdf.

Trevor Scott Standley, Amir Roshan Zamir, Dawn Chen, Leonidas J. Guibas, Jitendra Malik, and Silvio Savarese. Which tasks should be learned together in multi-task learning? In *ICML*, 2020.

Ximeng Sun, Rameswar Panda, Rogerio Feris, and Kate Saenko. Adashare: Learning what to share for efficient deep multi-task learning. In H. Larochelle, M. Ranzato, R. Hadsell, M.F. Balcan, and H. Lin (eds.), *Advances in Neural Information Processing Systems*, volume 33, pp. 8728–8740. Curran Associates, Inc., 2020. URL https://proceedings.neurips.cc/paper/2020/file/634841a6831464b64c072c8510c7f35c-Paper.pdf.

S. Vandenhende, S. Georgoulis, B. De Brabandere, and L. Van Gool. Branched Multi-Task Networks: Deciding What Layers To Share. In *BMVC*, 2020.

Simon Vandenhende, Stamatios Georgoulis, Wouter Van Gansbeke, Marc Proesmans, Dengxin Dai, and Luc Van Gool. Multi-task learning for dense prediction tasks: A survey. *IEEE transactions on pattern analysis and machine intelligence*, PP, 2021.

Hongyi Wang, Mikhail Yurochkin, Yuekai Sun, Dimitris Papailiopoulos, and Yasaman Khazaeni. Federated learning with matched averaging. In *International Conference on Learning Representations*, 2020a. URL https://openreview.net/forum?id=BkluqlSFDS.

Lijun Wang, Jianming Zhang, Oliver Wang, Zhe Lin, and Huchuan Lu. Sdc-depth: Semantic divide-and-conquer network for monocular depth estimation. In *Proceedings of the IEEE/CVF Conference on Computer Vision and Pattern Recognition*, pp. 541–550, 2020b.

Jingwen Ye, Yixin Ji, Xinchao Wang, Kairi Ou, Dapeng Tao, and Mingli Song. Student becoming the master: Knowledge amalgamation for joint scene parsing, depth estimation, and more. *2019 IEEE/CVF Conference on Computer Vision and Pattern Recognition (CVPR)*, pp. 2824–2833, 2019.

Changqian Yu, Changxin Gao, Jingbo Wang, Gang Yu, Chunhua Shen, and Nong Sang. Bisenet v2: Bilateral network with guided aggregation for real-time semantic segmentation. *International Journal of Computer Vision*, 129(11):3051–3068, 2021.

Tianhe Yu, Saurabh Kumar, Abhishek Gupta, Sergey Levine, Karol Hausman, and Chelsea Finn. Gradient surgery for multi-task learning. In H. Larochelle, M. Ranzato, R. Hadsell, M.F. Balcan, and H. Lin (eds.), *Advances in Neural Information Processing Systems*, volume 33, pp. 5824–5836. Curran Associates, Inc., 2020. URL https://proceedings.neurips.cc/paper/2020/file/3fe78a8acf5fda99de95303940a2420c-Paper.pdf.

Lijun Zhang, Xiao Liu, and Hui Guan. Automtl: A programming framework for automated multi-task learning, 2021.

Lijun Zhang, Xiao Liu, and Hui Guan. A tree-structured multi-task model recommender. In *First Conference on Automated Machine Learning (Main Track)*, 2022. URL https://openreview.net/forum?id=BEl4CgaHLlc.

# A ADDITIONAL RELATED WORKS

MTSL relies on local task similarity to drive group neuron creation and the removal of the corresponding task neurons. The learned convolutional filters in different task branches might not align one-on-one due to the permutation invariance of convolutional neural networks Wang et al. (2020a). Existing works Wang et al. (2020a); Leontev et al. (2019); Singh & Jaggi (2020); He et al. (2018) use different ways to align corresponding layers of two models to counteract the permutation invariance. MTSL uses CKA Kornblith et al. (2019) to align neurons based on representation similarity. Knowledge amalgamation approaches Li & Bilen (2020); Shen et al. (2019); Luo et al. (2020; 2019); He et al. (2018) address distilling the knowledge from multiple learned teachers into a single student. Ye et al. (2019) create task-specific coding at a layer in the student network using a small network for feature distillation. MTSL uses this feature distillation process to exploit the knowledge of the task neurons set to be removed.

# B GROUPING ALGORITHM

At the beginning of the structural learning phase, task nodes are grouped based on local similarity between task node features. The grouping algorithm used to provide this grouping decision is detailed in Algorithm 2. This algorithm provides the best possible task grouping which is subsequently used to determine creation of group nodes and removal of task nodes.

**Algorithm 2:** Grouping

**Input:** Task set $\mathcal{T}$ and Similarity $S_{ij}, i, j \in \mathcal{T}, i \neq j$;
Group $G \leftarrow \{\text{tasks}\}$;
Grouping $\mathcal{G} \leftarrow \{\text{groups}\}$;
Task value in group $G$ is $\mathcal{V}_t \leftarrow \frac{1}{i}\sum_i S_{ti}$, where $i \subset G \backslash t$;
Group value $\mathcal{V}_G \leftarrow \frac{1}{t}\sum_t \mathcal{V}_t$, where t is the #tasks in group ;
Unique Grouping $\mathbb{G} \subset \mathcal{G}$, such that all tasks are present exactly once;
**for** *all unique groupings* **do**
  $\mathcal{V}_{\mathbb{G}} \leftarrow \frac{1}{g}\sum_g \mathcal{V}_g$, where g is the #groups in grouping;
**end**
Final grouping $\leftarrow$ grouping with maximum $\mathcal{V}_{\mathbb{G}}$;
**Result:** Final grouping

# C ADDITIONAL TRAINING DETAILS

We provide additional training details to aid with reproducibility. CKA similarities for grouping decisions during training are calculated using a subset of 800 training images in Cityscapes and all 795 training images in NYUv2. The five tasks used in our experiments $\mathcal{S}$, $\mathcal{D}$, $\mathcal{E}$, $\mathcal{N}$, and $\mathcal{A}$ are evaluated with mIoU, RMSE, BCE (Binary Cross Entropy Error), Cosine Similarity, and MSE, respectively. The edge detection task $\mathcal{E}$ concerns the predictions of semantic edges in the scene. We use an encoder-decoder architecture where the first four layers of the encoder is initialized with the ImageNet pretrained weights while the last layer of the encoder and the decoder are initialized randomly.

Both for the baselines and MTSL, we use the same training hyperparameters and evaluation metrics. For training, we use the Adam optimizer with a learning rate of 1e-4 for 80 epochs. We use the step-wise learning schedule with steps at epochs 60 and 70. The batch size used is 16, a weight decay of 5e-5 and we equally weigh all task losses. In addition to averaging all parameters to initialize group node, we also average the optimizer state of the task nodes to get the optimizer state of group node. All other parameters that are not removed retain their weights as well as their optimizer state. The grouping threshold $\gamma$ used is 0.8 and the number of structural learning phases is set to 10. The task learning epochs for subsequent phases are 2, 2, 2, 2, 4, 4, 8, 8, 8, and 8 and knowledge amalgamation is done for 1, 1, 2, 2, 2, 2, 4, 4, 8, and 8 epochs in the subsequent structural learning phases. The task learning epochs and knowledge amalgamation epochs are increased progressively based on nature of task representations learnt at different stages of training. In early training, all the task nodes are in

early layers and need to learn low level features. Our intuition here is that these generic features are likely common across tasks and can be learnt fast. The former suggests our use of low epochs in the structural learning phase and the later the task learning phase early in the training. As we progress through the training, more epochs would be required to learn task specific features suggesting the increase in task specific phase epochs. Also, later in the training, features of each task likely diverge becoming more task specific suggesting the increase in structural learning phase epochs.

# D SENSITIVITY ANALYSIS

## D.1 SENSITIVITY OF THE CONVERGED ARCHITECTURES

In the main paper, we showed that the converged architecture differs between the two datasets Cityscapes and NYUv2. This suggests that the algorithm is sensitive to the dataset. In addition, we observe that the converged architectures are also sensitive to the initialization of the encoder and to random seeds. We tabulate the different architectures obtained in Table 5. The layer column lists the layers in the network and the corresponding entries in the remaining columns show what all tasks have been grouped. For instance, [$\mathcal{D}$, $\mathcal{N}$, $\mathcal{A}$] means $\mathcal{D}$, $\mathcal{N}$, and $\mathcal{A}$ are grouped together.

Table 5: Sensitivity of the converged architecture to different initialization of the encoder and random seeds in both datasets. The random seeds groupings using ImageNet pretrained weights for the encoder.

| | Layer | Seed 0 | Seed 1 | Seed 2 | Random Seed 2 |
|---|---|---|---|---|---|
| CS | 1-6 | [$\mathcal{S}$, $\mathcal{E}$, $\mathcal{D}$, $\mathcal{N}$, $\mathcal{A}$] | [$\mathcal{S}$, $\mathcal{E}$, $\mathcal{D}$, $\mathcal{N}$, $\mathcal{A}$] | [$\mathcal{S}$, $\mathcal{E}$, $\mathcal{D}$, $\mathcal{N}$, $\mathcal{A}$] | [$\mathcal{S}$, $\mathcal{E}$, $\mathcal{D}$, $\mathcal{N}$, $\mathcal{A}$] |
| | 7,8 | [$\mathcal{S}$, $\mathcal{E}$, $\mathcal{A}$], [$\mathcal{D}$, $\mathcal{N}$] | [$\mathcal{S}$, $\mathcal{E}$], [$\mathcal{D}$, $\mathcal{N}$, $\mathcal{A}$] | [$\mathcal{S}$, $\mathcal{E}$], [$\mathcal{D}$, $\mathcal{N}$, $\mathcal{A}$] | [$\mathcal{S}$, $\mathcal{E}$, $\mathcal{D}$, $\mathcal{N}$, $\mathcal{A}$] |
| | 9 | [$\mathcal{S}$, $\mathcal{E}$, $\mathcal{A}$], [$\mathcal{D}$], [$\mathcal{N}$] | [$\mathcal{S}$, $\mathcal{E}$], [$\mathcal{D}$], [$\mathcal{N}$], [$\mathcal{A}$] | [$\mathcal{S}$, $\mathcal{E}$], [$\mathcal{D}$, $\mathcal{N}$, $\mathcal{A}$] | [$\mathcal{S}$, $\mathcal{E}$, $\mathcal{D}$, $\mathcal{N}$, $\mathcal{A}$] |
| | 10 | [$\mathcal{S}$, $\mathcal{E}$, $\mathcal{A}$], [$\mathcal{D}$], [$\mathcal{N}$] | [$\mathcal{S}$, $\mathcal{E}$], [$\mathcal{D}$], [$\mathcal{N}$], [$\mathcal{A}$] | [$\mathcal{S}$, $\mathcal{E}$], [$\mathcal{D}$, $\mathcal{N}$], [$\mathcal{A}$] | [$\mathcal{S}$, $\mathcal{E}$, $\mathcal{D}$, $\mathcal{N}$, $\mathcal{A}$] |
| NYU | 1-6 | [$\mathcal{S}$, $\mathcal{E}$, $\mathcal{D}$, $\mathcal{N}$, $\mathcal{A}$] | [$\mathcal{S}$, $\mathcal{E}$, $\mathcal{D}$, $\mathcal{N}$, $\mathcal{A}$] | [$\mathcal{S}$, $\mathcal{E}$, $\mathcal{D}$, $\mathcal{N}$, $\mathcal{A}$] | [$\mathcal{S}$, $\mathcal{E}$, $\mathcal{D}$, $\mathcal{N}$, $\mathcal{A}$] |
| | 7,8,9 | [$\mathcal{S}$, $\mathcal{E}$], [$\mathcal{D}$, $\mathcal{N}$, $\mathcal{A}$] | [$\mathcal{S}$, $\mathcal{E}$, $\mathcal{N}$], [$\mathcal{D}$, $\mathcal{A}$] | [$\mathcal{S}$, $\mathcal{E}$], [$\mathcal{D}$, $\mathcal{N}$, $\mathcal{A}$] | [$\mathcal{S}$, $\mathcal{E}$, $\mathcal{D}$, $\mathcal{N}$, $\mathcal{A}$] |
| | 10 | [$\mathcal{S}$, $\mathcal{E}$], [$\mathcal{D}$], [$\mathcal{N}$], [$\mathcal{A}$] | [$\mathcal{S}$], [$\mathcal{E}$], [$\mathcal{N}$], [$\mathcal{D}$, $\mathcal{A}$] | [$\mathcal{S}$], [$\mathcal{E}$], [$\mathcal{D}$, $\mathcal{N}$, $\mathcal{A}$] | [$\mathcal{S}$, $\mathcal{E}$, $\mathcal{D}$, $\mathcal{N}$, $\mathcal{A}$] |

## D.2 SENSITIVITY TO GROUPING THRESHOLD

The grouping threshold determines whether or not a group of task nodes are similar enough to lead to the creation of a group node and eventual removal of the concerned task nodes. The sensitivity of MTSL to different grouping thresholds is shown in Table 6. A high grouping threshold would mean that task nodes are never grouped and the resultant architecture will be similar to STN in terms of GMac and parameters. However, the performance would still be different due to the use of CKA to regularize the task representations. A low grouping threshold would mean that task nodes are always grouped leading to architectures more similar to One-Net. We observe that for a threshold of 0.7 or less, MTSL leads to One-Net architecture but the performance is not sufficient. A threshold of 0.9 or higher leads to slow inference networks. A threshold of 0.8 provides the right trade-off and is used for all experiments in the main paper.

## D.3 SENSITIVITY TO NUMBER OF TASKS

We evaluate whether or not MTSL leads to improvements over One-Net when only 4 out of the 5 tasks is used. To this end, we train multi-task networks for 4 tasks namely $\mathcal{S}$, $\mathcal{E}$, $\mathcal{D}$ and $\mathcal{N}$. The results are tabulated in 7. We observe than even when there are 4 tasks, MTSL improves over One-Net.

# E RETRAINING THE CONVERGED ARCHITECTURES

We evaluate the effectiveness of the learned architecture with and without the learned parameters. The learned architecture is reinitialized and retrained under the same training settings as MTSL. The result of this retrained architecture is presented as MTSL-A in Table 8. Both MTSL-A and MTSL

Table 6: Sensitivity of MTSL to the grouping threshold. For example, MTSL-0.1 denotes MTSL with grouping threshold of 0.1. # (M) denotes the number of parameters in millions.

| | Network | $\mathcal{S}\uparrow$ | $\mathcal{D}\downarrow$ | $\mathcal{E}\downarrow$ | $\mathcal{N}\uparrow$ | $\mathcal{A}\downarrow$ | $\Delta_{MTL}^{\mathcal{SD}}\uparrow$ | $\Delta_{MTL}\uparrow$ | # (M) | GMac |
|---|---|---|---|---|---|---|---|---|---|---|
| CS | STN | 61.95 | 6.38 | 0.0341 | 0.6108 | 0.0535 | - | - | 107.10 | 31.03 |
| CS | One-Net | 60.02 | 6.71 | 0.0421 | 0.5941 | 0.0620 | -4.10 | -10.06 | 21.70 | 7.06 |
| CS | MTSL-0.1 | 59.98 | 6.75 | 0.0439 | 0.5955 | 0.0626 | -4.48 | -11.44 | 21.70 | 7.06 |
| CS | MTSL-0.2 | 59.97 | 6.68 | 0.0433 | 0.5956 | 0.0629 | -3.92 | -10.98 | 21.70 | 7.06 |
| CS | MTSL-0.3 | 59.97 | 6.70 | 0.0437 | 0.5961 | 0.0629 | -4.06 | -11.25 | 21.70 | 7.06 |
| CS | MTSL-0.4 | 60.32 | 6.67 | 0.0436 | 0.5960 | 0.0626 | -3.59 | -10.90 | 21.70 | 7.06 |
| CS | MTSL-0.5 | 59.95 | 6.68 | 0.0437 | 0.5963 | 0.0626 | -3.95 | -11.09 | 21.70 | 7.06 |
| CS | MTSL-0.6 | 60.31 | 6.72 | 0.0431 | 0.5967 | 0.0628 | -3.98 | -10.81 | 21.70 | 7.06 |
| CS | MTSL-0.7 | 59.48 | 6.68 | 0.0432 | 0.5965 | 0.0625 | -4.32 | -10.90 | 21.70 | 7.06 |
| CS | MTSL-0.8 | 60.64 | 6.52 | 0.0415 | 0.6023 | 0.0565 | -2.13 | -6.59 | 22.99 | 9.53 |
| CS | MTSL-0.9 | 60.04 | 6.46 | 0.0359 | 0.6074 | 0.0559 | -2.12 | -2.91 | 95.97 | 16.30 |
| CS | MTSL-1.0 | 60.73 | 6.46 | 0.0340 | 0.6105 | 0.0538 | -1.61 | -0.71 | 107.10 | 31.03 |
| NYU | STN | 35.36 | 52.36 | 0.0566 | 0.7966 | 0.1401 | - | - | 107.10 | 33.99 |
| NYU | One-Net | 33.99 | 53.26 | 0.0634 | 0.7378 | 0.1557 | -2.80 | -7.22 | 21.70 | 7.77 |
| NYU | MTSL-0.1 | 34.48 | 53.29 | 0.0634 | 0.7330 | 0.1859 | -2.13 | -11.39 | 21.70 | 7.77 |
| NYU | MTSL-0.2 | 33.99 | 52.95 | 0.0635 | 0.7328 | 0.1840 | -2.49 | -11.30 | 21.70 | 7.77 |
| NYU | MTSL-0.3 | 34.69 | 52.92 | 0.0638 | 0.7337 | 0.1824 | -1.48 | -10.75 | 21.70 | 7.77 |
| NYU | MTSL-0.4 | 34.07 | 53.23 | 0.0634 | 0.7346 | 0.1772 | -2.65 | -10.32 | 21.70 | 7.77 |
| NYU | MTSL-0.5 | 34.19 | 52.94 | 0.0633 | 0.7349 | 0.1861 | -2.20 | -11.36 | 21.70 | 7.77 |
| NYU | MTSL-0.6 | 34.27 | 53.07 | 0.0636 | 0.7360 | 0.1860 | -2.21 | -11.43 | 21.70 | 7.77 |
| NYU | MTSL-0.7 | 34.53 | 53.22 | 0.0638 | 0.7330 | 0.1888 | -2.00 | -11.89 | 21.70 | 7.77 |
| NYU | MTSL-0.8 | 34.63 | 52.81 | 0.0586 | 0.7309 | 0.1649 | -1.46 | -6.48 | 22.84 | 10.11 |
| NYU | MTSL-0.9 | 35.22 | 52.25 | 0.0587 | 0.7149 | 0.1504 | -0.10 | -4.30 | 95.97 | 17.87 |
| NYU | MTSL-1.0 | 35.71 | 52.88 | 0.0565 | 0.7921 | 0.1344 | 0.00 | 0.74 | 107.10 | 33.99 |

Table 7: Sensitivity of MTSL to number of tasks. # (M) denotes the number of parameters in millions.

| | Network | $\mathcal{S}\uparrow$ | $\mathcal{D}\downarrow$ | $\mathcal{E}\downarrow$ | $\mathcal{N}\uparrow$ | $\Delta_{MTL}^{\mathcal{SD}}\uparrow$ | $\Delta_{MTL}\uparrow$ | # (M) | GMac |
|---|---|---|---|---|---|---|---|---|---|
| CS | STN | 59.84 | 6.43 | 0.0341 | 0.6114 | - | - | 85.68 | 24.80 |
| CS | One-Net | 60.38 | 6.79 | 0.0415 | 0.5966 | -2.31 | -7.18 | 21.63 | 6.83 |
| CS | MTSL | **60.41** | **6.43** | **0.0360** | **0.6068** | **0.45** | **-1.35** | 77.33 | 13.75 |
| NYU | STN | 35.41 | 53.10 | 0.0572 | 0.7881 | - | - | 85.68 | 27.18 |
| NYU | One-Net | 34.37 | 53.29 | 0.0623 | **0.7427** | -1.65 | -4.49 | 21.63 | 7.51 |
| NYU | MTSL | **35.95** | **51.69** | **0.0585** | 0.7127 | **2.08** | **-1.92** | 77.33 | 15.09 |

Table 8: Generalization and robustness comparison of MTSL against a version where the learned architecture is reinitialized and retrained (MTSL-A).

| | Network | $\Delta^{\mathcal{SD}}_{MTL} \uparrow$ | $\Delta_{MTL} \uparrow$ | $\Delta^{\mathcal{SD}}_{MTL} \uparrow$ | | | | $\Delta_{MTL} \uparrow$ | | | |
|---|---|---|---|---|---|---|---|---|---|---|---|
| | | Generalization | | N | B | W | D | N | B | W | D |
| CS | One-Net | -3.47 | -9.65 | -5.78 | -1.32 | -3.81 | -2.15 | +3.02 | -7.73 | -1.36 | -12.22 |
| | MTSL-A | **-1.22** | **-6.71** | -3.49 | +0.15 | -4.64 | +0.51 | **+4.50** | -4.13 | +0.23 | -8.33 |
| | MTSL | -1.35 | -7.04 | **-3.03** | **+0.21** | **+0.49** | **+1.42** | +2.92 | **-3.72** | **+2.60** | **-7.07** |
| NYU | One-Net | -2.77 | -9.82 | **+10.25** | -3.71 | -3.27 | -2.72 | +15.72 | -8.51 | -11.79 | -10.35 |
| | MTSL-A | -1.34 | -6.71 | +7.25 | **-1.84** | -2.29 | -1.42 | **+15.92** | **-7.16** | **+3.31** | -7.72 |
| | MTSL | **+0.06** | **-6.21** | +1.92 | -2.65 | **-0.84** | **-1.14** | +13.50 | -8.03 | +3.22 | **-7.54** |

Table 9: Switching the converged architectures. # (M) denotes the number of parameters in millions.

| | Network | $\mathcal{S} \uparrow$ | $\mathcal{D} \downarrow$ | $\mathcal{E} \downarrow$ | $\mathcal{N} \uparrow$ | $\mathcal{A} \downarrow$ | $\Delta^{\mathcal{SD}}_{MTL} \uparrow$ | $\Delta_{MTL} \uparrow$ | # (M) | GMac |
|---|---|---|---|---|---|---|---|---|---|---|
| CS | STN | 61.95 | 6.38 | 0.0341 | 0.6108 | 0.0535 | - | - | 107.10 | 31.03 |
| | One-Net | 60.02 | 6.71 | 0.0421 | 0.5941 | 0.0620 | -4.10 | -10.06 | 21.70 | 7.06 |
| | MTSL-A | 60.34 | 6.46 | 0.0414 | 0.6028 | 0.0567 | -1.92 | -6.51 | 22.99 | 9.53 |
| | MTSL-A-Switch | 61.30 | 6.54 | 0.0380 | 0.5987 | 0.0569 | -1.78 | -4.67 | 22.83 | 9.20 |
| NYU | STN | 35.36 | 52.36 | 0.0566 | 0.7966 | 0.1401 | - | - | 107.10 | 33.99 |
| | One-Net | 33.99 | 53.26 | 0.0634 | 0.7378 | 0.1557 | -2.80 | -7.22 | 21.70 | 7.77 |
| | MTSL-A | 34.94 | 52.89 | 0.0585 | 0.7342 | 0.1524 | -1.10 | -4.43 | 22.84 | 10.11 |
| | MTSL-A-Switch | 35.25 | 52.66 | 0.0628 | 0.7308 | 0.1561 | -0.44 | -6.30 | 22.90 | 10.47 |

provide improved results when compared with One-Net suggesting that both the learned architecture in and of itself and the MTSL training procedure of simultaneously learning the architecture and its parameters are beneficial.

Next, we provide results for MTSL-A where the converged architectures are retrained from scratch. Instead of retraining the architecture converged on a dataset to retrain on the same dataset, we use the converged architecture in Cityscapes to train on NYUv2 and vice versa. We refer to this switched evaluation as MTSL-A-Switch. The results are provided in Table 9. We observe that switching the converged architectures leads to marginal improvements.

## F Additional similarity metric

Instead of using CKA for alignment and grouping, a variety of other similarity metrics can be used. Here, we replace CKA with Representation Similarity Analysis (RSA) and provide the results in Table 10. We observe that RSA is able to improve the results of MTSL but at the cost of additional computation.

Table 10: MTSL with a different similarity metric called RSA. # (M) denotes the number of parameters in millions.

| | Network | $\mathcal{S} \uparrow$ | $\mathcal{D} \downarrow$ | $\mathcal{E} \downarrow$ | $\mathcal{N} \uparrow$ | $\mathcal{A} \downarrow$ | $\Delta^{\mathcal{SD}}_{MTL} \uparrow$ | $\Delta_{MTL} \uparrow$ | # (M) | GMac |
|---|---|---|---|---|---|---|---|---|---|---|
| CS | STN | $60.87_{\pm 0.78}$ | $6.37_{\pm 0.02}$ | $0.03_{\pm 0.00}$ | $0.61_{\pm 0.00}$ | $0.05_{\pm 0.00}$ | - | - | 107.10 | 31.03 |
| | MTSL | $\mathbf{60.68}_{\pm 0.10}$ | $6.52_{\pm 0.03}$ | $\mathbf{0.04}_{\pm 0.00}$ | $0.60_{\pm 0.00}$ | $\mathbf{0.06}_{\pm 0.00}$ | $-1.35_{\pm 0.70}$ | $-7.04_{\pm 0.56}$ | 22.86 | 8.96 |
| | MTSL-RSA | $60.61_{\pm 0.39}$ | $\mathbf{6.43}_{\pm 0.05}$ | $\mathbf{0.04}_{\pm 0.00}$ | $\mathbf{0.61}_{\pm 0.00}$ | $\mathbf{0.06}_{\pm 0.00}$ | $\mathbf{-0.72}_{\pm 0.61}$ | $\mathbf{-2.36}_{\pm 0.18}$ | 95.97 | 16.3 |
| NYU | STN | $35.63_{\pm 0.53}$ | $52.70_{\pm 0.25}$ | $0.06_{\pm 0.00}$ | $0.80_{\pm 0.00}$ | $0.14_{\pm 0.00}$ | - | - | 107.10 | 33.99 |
| | MTSL | $\mathbf{35.50}_{\pm 0.25}$ | $52.46_{\pm 0.23}$ | $\mathbf{0.06}_{\pm 0.00}$ | $\mathbf{0.73}_{\pm 0.00}$ | $0.16_{\pm 0.00}$ | $+0.06_{\pm 1.03}$ | $-6.21_{\pm 0.90}$ | 22.81 | 9.89 |
| | MTSL-RSA | $\mathbf{35.50}_{\pm 0.20}$ | $\mathbf{52.19}_{\pm 0.12}$ | $\mathbf{0.06}_{\pm 0.00}$ | $0.71_{\pm 0.00}$ | $\mathbf{0.15}_{\pm 0.00}$ | $\mathbf{+0.31}_{\pm 0.54}$ | $\mathbf{-4.77}_{\pm 0.53}$ | 95.97 | 16.3 |

Table 11: Generalization and inference efficiency comparisons between MTSL and state-of-the-art methods namely Cross-stitch Misra et al. (2016), MTAN Liu et al. (2019), LTB Guo et al. (2020) and BMTAS Bruggemann et al. (2020). LTB-R and BMTAS-R denote the results obtained by retraining the converged models of LTB and BMTAS. In MTSL-RSA, the similarity metric CKA is replaced with RSA. # (M) denotes the number of parameters in millions.

| | Network | $\mathcal{S} \uparrow$ | $\mathcal{D} \downarrow$ | $\mathcal{E} \downarrow$ | $\mathcal{N} \uparrow$ | $\mathcal{A} \downarrow$ |
|---|---|---|---|---|---|---|
| CS | STN | $50.77_{\pm 0.18}$ | $7.22_{\pm 0.01}$ | 0.0642 | 0.5819 | 0.2246 |
| | One-Net | $50.90_{\pm 0.13}$ | $7.36_{\pm 0.03}$ | $0.0650_{\pm 0.00}$ | $0.5783_{\pm 0.00}$ | $0.2302_{\pm 0.00}$ |
| | Cross-stitch | $52.63_{\pm 0.34}$ | $7.08_{\pm 0.01}$ | $0.0644_{\pm 0.00}$ | $0.5818_{\pm 0.00}$ | $0.2250_{\pm 0.00}$ |
| | MTAN | $51.41_{\pm 0.63}$ | $7.31_{\pm 0.01}$ | $0.0650_{\pm 0.00}$ | $0.5805_{\pm 0.00}$ | $0.2626_{\pm 0.00}$ |
| | LTB | $49.57_{\pm 0.47}$ | $7.47_{\pm 0.02}$ | $0.0649_{\pm 0.00}$ | $0.5812_{\pm 0.00}$ | $0.2289_{\pm 0.00}$ |
| | LTB-R | $51.29_{\pm 0.28}$ | $7.22_{\pm 0.03}$ | $0.0643_{\pm 0.00}$ | $0.5820_{\pm 0.00}$ | $0.2253_{\pm 0.00}$ |
| | BMTAS | $48.84_{\pm 0.29}$ | $7.50_{\pm 0.03}$ | $0.0649_{\pm 0.00}$ | $0.5809_{\pm 0.00}$ | $0.2290_{\pm 0.00}$ |
| | BMTAS-R | $51.18_{\pm 0.32}$ | $7.24_{\pm 0.06}$ | $0.0644_{\pm 0.00}$ | $0.5820_{\pm 0.00}$ | $0.2253_{\pm 0.00}$ |
| | MTSL | $50.81_{\pm 0.59}$ | $7.26_{\pm 0.03}$ | $0.0644_{\pm 0.00}$ | $0.5820_{\pm 0.00}$ | $0.2268_{\pm 0.00}$ |
| | MTSL-RSA | $51.10_{\pm 0.20}$ | $7.18_{\pm 0.02}$ | $0.0644_{\pm 0.00}$ | $0.5819_{\pm 0.00}$ | $0.2254_{\pm 0.00}$ |
| NYU | STN | $34.56_{\pm 0.19}$ | $54.17_{\pm 0.17}$ | $0.0764_{\pm 0.00}$ | $0.7712_{\pm 0.00}$ | $0.5933_{\pm 0.00}$ |
| | One-Net | $33.49_{\pm 0.38}$ | $53.35_{\pm 0.29}$ | $0.0776_{\pm 0.00}$ | $0.7041_{\pm 0.00}$ | $0.6590_{\pm 0.00}$ |
| | Cross-stitch | $34.25_{\pm 0.23}$ | $52.90_{\pm 0.24}$ | $0.0768_{\pm 0.00}$ | $0.7010_{\pm 0.00}$ | $0.6096_{\pm 0.00}$ |
| | MTAN | $33.79_{\pm 0.51}$ | $53.33_{\pm 0.27}$ | $0.0764_{\pm 0.00}$ | $0.7070_{\pm 0.00}$ | $0.6563_{\pm 0.00}$ |
| | LTB | $31.92_{\pm 0.04}$ | $55.21_{\pm 0.22}$ | $0.0768_{\pm 0.00}$ | $0.6964_{\pm 0.00}$ | $0.6345_{\pm 0.00}$ |
| | LTB-R | $34.04_{\pm 0.47}$ | $53.49_{\pm 0.40}$ | $0.0768_{\pm 0.00}$ | $0.7725_{\pm 0.00}$ | $0.5970_{\pm 0.00}$ |
| | BMTAS | $32.09_{\pm 0.29}$ | $54.64_{\pm 0.36}$ | $0.0768_{\pm 0.00}$ | $0.6978_{\pm 0.00}$ | $0.6370_{\pm 0.00}$ |
| | BMTAS-R | $34.30_{\pm 0.26}$ | $53.88_{\pm 0.12}$ | $0.0764_{\pm 0.00}$ | $0.7685_{\pm 0.00}$ | $0.5968_{\pm 0.00}$ |
| | MTSL | $33.83_{\pm 0.30}$ | $53.09_{\pm 0.11}$ | $0.0776_{\pm 0.00}$ | $0.6993_{\pm 0.00}$ | $0.6233_{\pm 0.00}$ |
| | MTSL-RSA | $33.74_{\pm 0.33}$ | $53.33_{\pm 0.31}$ | $0.0768_{\pm 0.00}$ | $0.7047_{\pm 0.00}$ | $0.6271_{\pm 0.00}$ |

## G EXTENDED NUMBERS FOR COMPARISON WITH SOTA

Table 11 provides extended numbers for all the sota method against which MTSL is compared.

## H ROBUSTNESS TO ADVERSARIAL ATTACK

In addition to the robustness to natural corruptions discussed in the main paper, we evaluate the robustness to PGD attacks Madry et al. (2018). We perform the attacks using four epsilon levels (0.25, 0.5, 1 and 2), step size of 1 and number of iterations determined using $\min(\epsilon + 4, \lceil 1.25\epsilon \rceil)$ (Kurakin et al., 2017). For each task $\mathcal{S}$ and $\mathcal{D}$, the corresponding task loss is used for attack. MTSL provides improved robustness over One-Net in most cases.

## I EXTENDED NUMBER FOR GENERALIZATION RESULTS

The generalization performance of the baselines and MTSL have been provided in Table 13 with extended digits after the decimal point where required.

## J EXTENDED NUMBERS FOR ABLATION RESULTS

The performance of each task while using different components of MTSL is provided in Table 14.

Table 12: Robustness to PGD attack of the baselines, MTSL-A and MTSL.

| | Network | $\mathcal{S}\uparrow$ | | | | $\mathcal{D}\downarrow$ | | | |
|---|---|---|---|---|---|---|---|---|---|
| | | 0.25 | 0.5 | 1 | 2 | 0.25 | 0.5 | 1 | 2 |
| CS | STN | 45.42 | 40.76 | 31.14 | 24.56 | 10.80 | 13.21 | 19.93 | 25.86 |
| | One-Net | 45.28 | 40.97 | 31.41 | 24.84 | 11.63 | 14.42 | 22.16 | 29.04 |
| | MTSL | **46.42** | **41.72** | **31.94** | **25.34** | **11.28** | **14.02** | **21.52** | **28.58** |
| NYU | STN | 21.58 | 17.96 | 11.65 | 8.24 | 85.98 | 103.13 | 150.55 | 194.52 |
| | One-Net | 20.75 | 17.31 | 11.17 | 7.83 | 85.40 | 103.67 | 149.12 | **191.13** |
| | MTSL | **21.88** | **18.25** | **11.50** | **7.90** | **85.00** | **102.85** | **148.80** | 191.21 |

Table 13: Generalization comparisons between MTSL and the baselines. # (M) denotes the number of parameters in millions.

| | Network | $\mathcal{S}\uparrow$ | $\mathcal{D}\downarrow$ | $\mathcal{E}\downarrow$ | $\mathcal{N}\uparrow$ | $\mathcal{A}\downarrow$ |
|---|---|---|---|---|---|---|
| CS | STN | $60.87_{\pm 0.78}$ | $6.37_{\pm 0.02}$ | $0.0342_{\pm 0.00}$ | $0.6106_{\pm 0.00}$ | $0.0535_{\pm 0.00}$ |
| | One-Net | $60.34_{\pm 0.37}$ | $6.76_{\pm 0.04}$ | $0.0423_{\pm 0.00}$ | $0.5943_{\pm 0.00}$ | $0.0616_{\pm 0.00}$ |
| | One-Net-L | $60.71_{\pm 0.21}$ | $6.75_{\pm 0.03}$ | $0.0421_{\pm 0.00}$ | $0.5942_{\pm 0.00}$ | $0.0615_{\pm 0.00}$ |
| | MTSL | $\mathbf{60.68}_{\pm 0.10}$ | $\mathbf{6.52}_{\pm 0.03}$ | $\mathbf{0.0419}_{\pm 0.00}$ | $\mathbf{0.6029}_{\pm 0.00}$ | $\mathbf{0.0583}_{\pm 0.00}$ |
| NYU | STN | $35.63_{\pm 0.53}$ | $52.70_{\pm 0.25}$ | $0.0570_{\pm 0.00}$ | $0.7955_{\pm 0.00}$ | $0.1355_{\pm 0.00}$ |
| | One-Net | $34.15_{\pm 0.15}$ | $53.44_{\pm 0.39}$ | $0.0636_{\pm 0.00}$ | $\mathbf{0.7370}_{\pm 0.00}$ | $0.1688_{\pm 0.01}$ |
| | One-Net-L | $34.42_{\pm 0.17}$ | $53.36_{\pm 0.31}$ | $0.0634_{\pm 0.00}$ | $\mathbf{0.7366}_{\pm 0.00}$ | $0.1682_{\pm 0.01}$ |
| | MTSL | $\mathbf{35.50}_{\pm 0.25}$ | $\mathbf{52.46}_{\pm 0.23}$ | $\mathbf{0.0595}_{\pm 0.00}$ | $0.7298_{\pm 0.00}$ | $\mathbf{0.1605}_{\pm 0.00}$ |

Table 14: Ablation results of different tasks.

| | Align | Avg | ATT | $\mathcal{S}\uparrow$ | $\mathcal{D}\downarrow$ | $\mathcal{E}\downarrow$ | $\mathcal{N}\uparrow$ | $\mathcal{A}\downarrow$ |
|---|---|---|---|---|---|---|---|---|
| CS | | ✓ | | $60.54_{\pm 1.06}$ | $6.38_{\pm 0.02}$ | $0.0362_{\pm 0.00}$ | $0.6070_{\pm 0.00}$ | $0.0558_{\pm 0.00}$ |
| | | | ✓ | $61.13_{\pm 0.10}$ | $6.40_{\pm 0.05}$ | $0.0359_{\pm 0.00}$ | $0.6073_{\pm 0.00}$ | $0.0557_{\pm 0.00}$ |
| | | ✓ | ✓ | $60.95_{\pm 0.34}$ | $6.43_{\pm 0.02}$ | $0.0358_{\pm 0.00}$ | $0.6075_{\pm 0.00}$ | $0.0560_{\pm 0.00}$ |
| | ✓ | ✓ | | $60.29_{\pm 1.32}$ | $6.60_{\pm 0.13}$ | $0.0421_{\pm 0.00}$ | $0.6006_{\pm 0.00}$ | $0.0584_{\pm 0.00}$ |
| | ✓ | | ✓ | $59.39_{\pm 1.39}$ | $6.67_{\pm 0.11}$ | $0.0436_{\pm 0.00}$ | $0.5974_{\pm 0.00}$ | $0.0596_{\pm 0.00}$ |
| | ✓ | ✓ | ✓ | $60.68_{\pm 0.10}$ | $6.52_{\pm 0.03}$ | $0.0419_{\pm 0.00}$ | $0.6029_{\pm 0.00}$ | $0.0583_{\pm 0.00}$ |
| NYU | | ✓ | | $35.34_{\pm 0.06}$ | $51.88_{\pm 0.06}$ | $0.0589_{\pm 0.00}$ | $0.7145_{\pm 0.00}$ | $0.1470_{\pm 0.00}$ |
| | | | ✓ | $35.54_{\pm 0.44}$ | $51.97_{\pm 0.47}$ | $0.0590_{\pm 0.00}$ | $0.7140_{\pm 0.00}$ | $0.1469_{\pm 0.00}$ |
| | | ✓ | ✓ | $35.64_{\pm 0.50}$ | $52.40_{\pm 0.07}$ | $0.0589_{\pm 0.00}$ | $0.7102_{\pm 0.00}$ | $0.1461_{\pm 0.00}$ |
| | ✓ | ✓ | | $34.80_{\pm 0.33}$ | $52.80_{\pm 0.06}$ | $0.0584_{\pm 0.00}$ | $0.7331_{\pm 0.00}$ | $0.1634_{\pm 0.00}$ |
| | ✓ | | ✓ | $34.18_{\pm 0.44}$ | $53.05_{\pm 0.21}$ | $0.0588_{\pm 0.00}$ | $0.7344_{\pm 0.00}$ | $0.1599_{\pm 0.02}$ |
| | ✓ | ✓ | ✓ | $35.50_{\pm 0.25}$ | $52.46_{\pm 0.23}$ | $0.0595_{\pm 0.00}$ | $0.7298_{\pm 0.00}$ | $0.1605_{\pm 0.00}$ |